Determination of the Er^{3+} to Yb^{3+} energy transfer efficiency in Er^{3+}/Yb^{3+}-codoped YVO_4 crystals

2001 J. Phys.: Condens. Matter 13 7999

(http://iopscience.iop.org/0953-8984/13/35/307)

INSTITUTE OF PHYSICS PUBLISHING JOURNAL OF PHYSICS: CONDENSED MATTER

J. Phys.: Condens. Matter **13** (2001) 7999–8006 PII: S0953-8984(01)24548-2

Determination of the Er^{3+} to Yb^{3+} energy transfer efficiency in Er^{3+}/Yb^{3+}-codoped YVO_4 crystals

R E Di Paolo[1,2], E Cantelar[1], X M Wang[3], T Tsuboi[4] and F Cussó[1]

[1] Departamento de Física de Materiales, C-IV, Universidad Autónoma de Madrid, 28049 Madrid, Spain
[2] Centro de Investigaciones Ópticas (CIOp), CC 124, 1900 La Plata, Argentina
[3] Institute of Physics, Chinese Academy of Sciences, Beijing 100080, People's Republic of China
[4] Faculty of Engineering, Kyoto Sangyo University, Kamigamo, Kita-ku, Kyoto 603-8555, Japan

E-mail: fernando.cusso@uam.es

Received 3 May 2001, in final form 2 July 2001
Published 16 August 2001
Online at stacks.iop.org/JPhysCM/13/7999

Abstract

The energy transfer efficiency from Er^{3+} to Yb^{3+} ions in yttrium orthovanadate single crystals (YVO_4) is experimentally obtained, by using a method based on the simultaneous and multiwavelength measurement of photoacoustic and luminescent signals after pulsed laser excitation. The result is reached by comparing with the predictions from Judd–Ofelt analysis and the lifetime measurements. The energy transfer between the ions, from Er^{3+} to Yb^{3+}, must be considered in order to fit the experimental results. A value of energy transfer efficiency ($\Psi = 0.16$) is obtained.

1. Introduction

An yttrium orthovanadate single crystal (YVO_4) doped with rare-earth ions is an attractive material, that allows the incorporation of high concentrations of rare-earth ions and its use as a host material for microchip lasers. It is also an easy crystal to handle and has a strong birefringence that ensures the polarization state of emitted light. In particular, YVO_4:Nd^{3+} has been shown to be capable of handling high pump powers and it has a high emission cross section for high cw power [1].

The sensitization of rare-earth doped laser materials with Yb^{3+} is a well known method for increasing the optical pump efficiency because of the highly efficient energy transfer from Yb^{3+} to rare-earth ions [2, 3]. The Yb^{3+} ion exhibits a strong and broad absorption band at about 960 nm and can easily be pumped with infrared laser diodes that are commercially available, giving rise to up-conversion in the visible spectral region. The up-conversion of Er^{3+}/Yb^{3+} co-doped YVO_4 has been studied, and recently the spectroscopic properties, up-conversion and down-conversion, of Er^{3+}/Yb^{3+} co-doped YVO_4 were investigated [4, 5]. Nevertheless, in order to exploit the potentialities of this material, it is necessarily a better quantification

of the transfer parameters, and in particular, the Er^{3+} to Yb^{3+} energy transfer rate, which is important for application involving high density of photons/excited states, for instance in laser applications.

In this work, we present a comparative photoacoustic and luminescent study of the de-excitation efficiency of the green emission of erbium ions. The results show that for Er^{3+}/Yb^{3+} co-doped crystals, with high Yb^{3+} ion concentration, an energy transfer process from Er^{3+} to Yb^{3+} ions is operative. The measured lifetimes for two crystals with different rare-earth concentrations show a behaviour in agreement with this transfer process. The efficiency of this energy transfer was obtained using simultaneously luminescence and photoacoustic techniques, under pulsed dual-wavelength laser excitation [6–8].

2. Experiment

Single crystals of YVO_4 doped with Er^{3+} and Yb^{3+} have been grown using the floating-zone method at the Chinese Academy of Sciences, Beijing. Two crystals were grown: one contains 10 at.% Yb^{3+} and 1 at.% Er^{3+} in the melt, while the other contains 3 at.% Yb^{3+} and 0.3 at.% Er^{3+}.

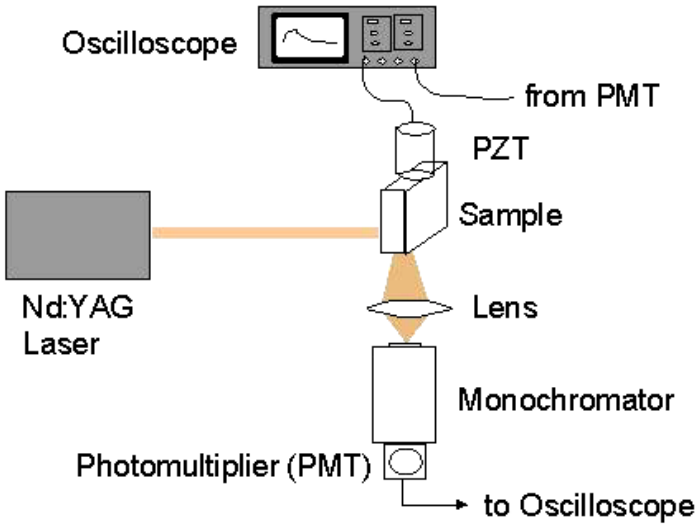

Figure 1. Experimental set-up used for the simultaneous measurement of photoacoustic and luminescence signals.

Photoacoustic and luminescence signals were measured simultaneously under the same pulsed excitation from a Nd:YAG laser. The experimental set-up is shown in figure 1. Photoacoustic signals (PAS) were detected by using a resonant piezoelectric transducer (PZT) [10]. The fluorescence was analysed through an ARC monochromator model SpectraPro 500-I and then detected synchronously with a photomultiplier tube (Hamamatsu R928) and recorded by a digital oscilloscope (Tektronics 420). In order to improve the signal-to-noise ratio, the photoacoustic signals were recorded by using a temporal window of the digital oscilloscope, which selected the first ten microseconds from the signal after the excitation. Additionally, PAS was averaged over 200 pulses of excitation and this measurement repeated ten times. In this way the effects in the signals caused by some energy-pulse instability could be eliminated.

Lifetime measurements were obtained at room temperature, under pulsed excitation using a Nd:YAG laser (532 nm, second harmonic). The temporal resolution of the system was limited by the laser pulse width (10 ns). Geometry for luminescence collection has been ensured in order to avoid radiation trapping effects that would generate a lengthening in the lifetime measurements [9].

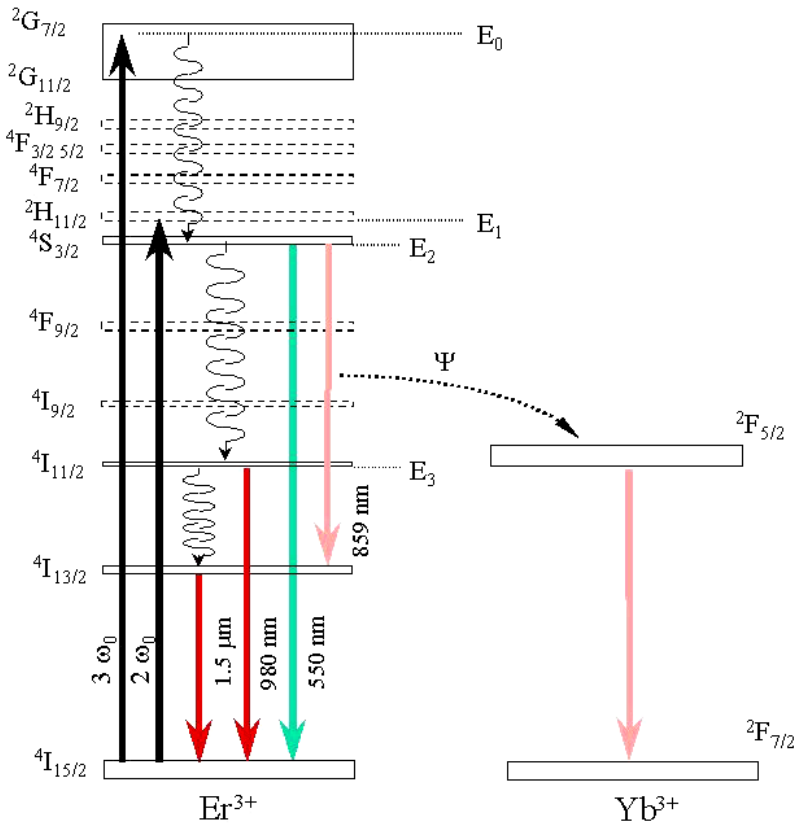

Figure 2. Schematic energy level diagram of YVO_4:Er^{3+}/Yb^{3+} showing the multiplets involved in the energy transfer processes studied (dotted line) as well as the dominant emissions.

3. Results and discussion

The energy level diagram of Er^{3+}/Yb^{3+} ions is shown in figure 2. After optical excitation to the upper energy levels, the main luminescent emissions of Er^{3+} appear in the infrared, 1.5 μm and 980 nm, associated with $^4I_{13/2} \rightarrow {}^4I_{15/2}$ and $^4I_{11/2} \rightarrow {}^4I_{15/2}$ transition respectively, and in the green (550 nm) associated with the $^4S_{3/2}$, $^2H_{11/2} \rightarrow {}^4I_{15/2}$ transition [4]. It is possible also to detect luminescence at 859 nm, associated with the $^4S_{3/2} \rightarrow {}^4I_{13/2}$ transition, but much weaker than the emissions mentioned above. All remaining excited states have negligibly small contributions to the luminescence spectrum, decaying non-radiatively to the lower lying levels.

When Er^{3+} ions are excited with the third ($3\omega_0$) harmonics of the Nd:YAG laser, leading initially to the $^2G_{7/2}$ level (see figure 2), a non-radiative multiphonon relaxation occurs, reaching finally the $^4S_{3/2}$ level. This level is also reached from the $^2H_{11/2}$ when the excitation is performed by using the second ($2\omega_0$) harmonics of the Nd:YAG laser. It is worth noting

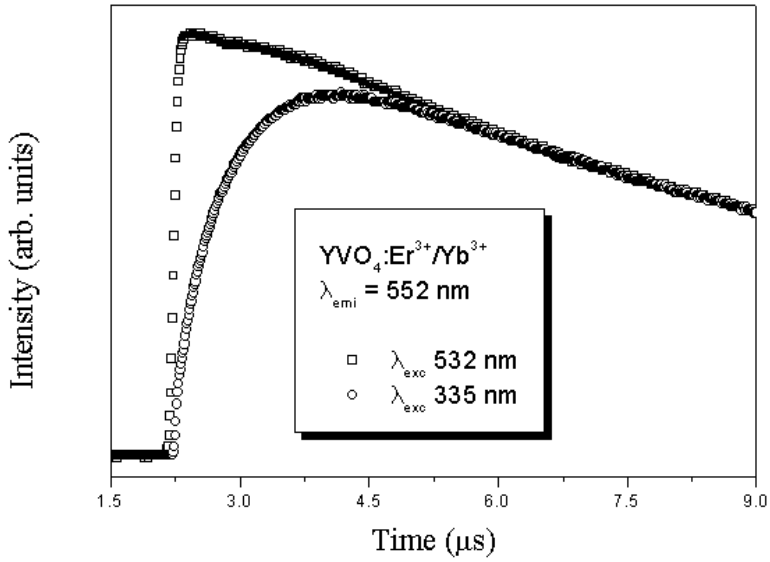

Figure 3. Temporal evolution (in a logarithmic scale) of the green luminescence of Er^{3+} ions ($^4S_{3/2}$, $^2H_{11/2} \rightarrow {}^4I_{15/2}$), measured at 552 nm, after pulsed excitation of the Er^{3+} ions at 355 nm and 532 nm, for the sample co-doped with 10 at.% Yb^{3+} and 1 at.% Er^{3+}.

that upon $3\omega_0$ excitation a weak but non-negligible fluorescence was observed at 380 nm. This is attributed to the $^2G_{11/2} \rightarrow {}^4I_{15/2}$ transition. The observed lifetime for this transition is significantly shorter than the calculated radiative lifetime, indicating that non-radiative processes dominate the decay. Figure 3 allows us to observe different rise times of the luminescence, indicating different dynamic population of the $^4S_{3/2}$ level depending on the excitation wavelength. A representation in logarithmic scale of the lifetime measurements shows the exponential decays as straight lines.

From the $^4S_{3/2}$ level the same decaying cascade follows, independently of whether the initial excitation has occurred at $2\omega_0$ or $3\omega_0$, with a characteristic lifetime of $\tau = 9$ μs at room temperature (figure 4). The situation is therefore similar to that found in Er^{3+} in lithium niobate [8], which allows the determination of absolute quantum efficiencies by using the non-radiative de-excitation as an internal reference for calibration.

After pulsed excitation with the Nd:YAG laser, the green luminescence of the $^4S_{3/2} \rightarrow {}^4I_{15/2}$ transition and the photoacoustic signal are simultaneously measured.

Taking into account all levels and the transitions involved and considering that all processes originating from the $^4I_{11/2}$ and $^4I_{13/2}$ levels (characteristic lifetimes 202 μs and 3 ms respectively) correspond to a temporal range out of the temporal window of sampling, and then they do not contribute to the observed photoacoustic response, the photoacoustic and luminescence signals can be expressed as

$$\mathrm{LUMS}(2\omega_0) = K_L \Phi N(2\omega_0) \tag{1a}$$

$$\mathrm{LUMS}(3\omega_0) = K_L \Phi N(3\omega_0) \tag{1b}$$

$$\mathrm{PAS}(2\omega_0) = K_P N(2\omega_0)[(E_1 - E_2) + (1 - \Phi)(E_2 - E_3)] \tag{1c}$$

$$\mathrm{PAS}(3\omega_0) = K_P N(3\omega_0)[(E_0 - E_2) + (1 - \Phi)(E_2 - E_3)] \tag{1d}$$

where $N(2\omega_0, 3\omega_0)$ indicates the number of absorbed photons by the Er^{3+} ions at the corresponding excitation, K_L and K_P are the proportionality constants that include all

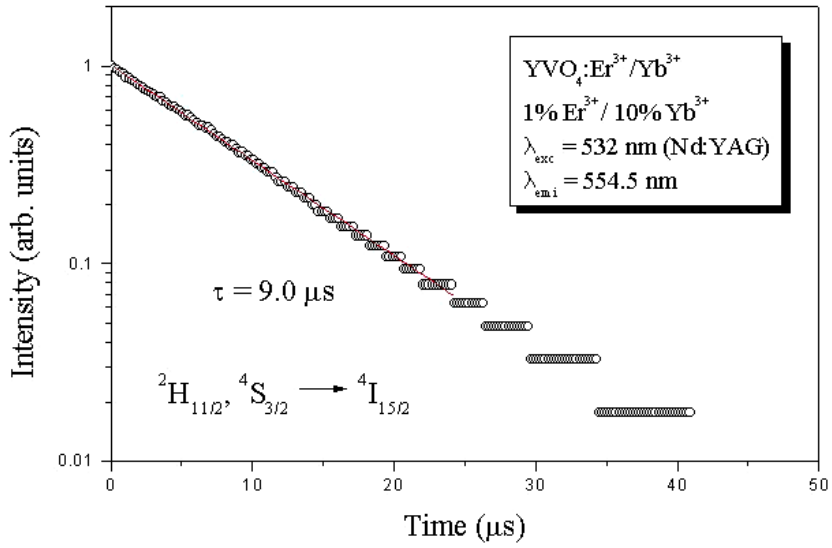

Figure 4. Temporal evolution of the green luminescence of Er^{3+} ions ($^4S_{3/2}$, $^2H_{11/2} \rightarrow {}^4I_{15/2}$), measured at 554.5 nm, after pulsed excitation of the Er^{3+} ions at 532 nm, for the sample co-doped with 10 at.% Yb^{3+} and 1 at.% Er^{3+} (open circles). The line corresponds to the fitting of the decay with a straight line.

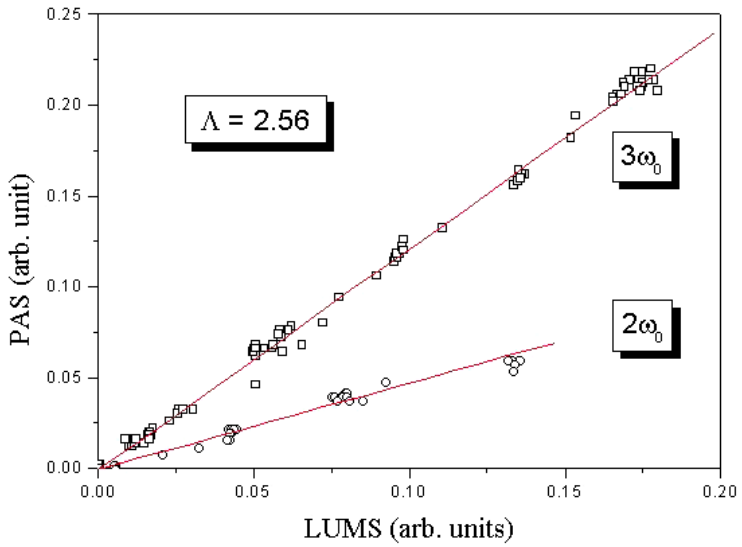

Figure 5. Comparison of photoacoustic (PAS)–luminescence (LUMS) signals simultaneously generated after $3\omega_0$ ($\lambda_{exc} = 355$ nm) and $2\omega_0$ ($\lambda_{exc} = 532$ nm) excitation for Er^{3+}/Yb^{3+} in YVO_4. In each case, the quotient between both signals is fitted with a straight line.

the instrumental responses in the collection of luminescence and photoacoustic signals respectively. Φ is the luminescence quantum efficiency of the $^4S_{3/2}$ level.

Figure 5 shows the comparison of the photoacoustic and luminescence signals for a series of excitations performed at different pump energies from the excitation laser. For that purpose

the laser beam was attenuated using neutral filters and the pump power was varied from 1 mJ to 20 mJ. A linear dependence between photoacoustic and luminescence signals is observed in accordance with equations (1*a*)–(1*d*). The difference in slope between $2\omega_0$ and $3\omega_0$ excitation is a consequence of the non-radiative connection between the state excited of Er^{3+} ions.

Equations (1*a*)–(1*d*) can be conveniently rearranged and the constants K_L and K_P eliminated, leading to the expression

$$\Phi = \frac{\Lambda(E_1 - E_3) - (E_0 - E_3)}{(\Lambda - 1)(E_2 - E_3)} \tag{2}$$

where

$$\Lambda = \frac{\mathrm{PAS}(3\omega_0)/\mathrm{LUMS}(3\omega_0)}{\mathrm{PAS}(2\omega_0)/\mathrm{LUMS}(2\omega_0)} \tag{3}$$

is the quantity to be experimentally determined.

From the least squares fitting of the experimental results given in figure 5, a ratio of slopes $\Lambda = 2.56 \pm 0.1$ is calculated, and finally from equation (2) a value $\Phi = 0.31 \pm 0.05$ is obtained.

This value can be compared with the predictions from the ratio between experimental lifetime (τ_{exp}) and the radiative lifetime (τ_{rad}) calculated from Judd–Ofelt theory ($\Phi = \tau_{exp}/\tau_{rad}$). In order to do that it is necessary to consider that the energy separation between the $^4S_{3/2}$ and $^2H_{11/2}$ levels, as obtained from the absorption spectrum, is small enough that these two levels are thermalized at room temperature. As the transition probability of the $^2H_{11/2}$ level is substantially higher than that of the $^4S_{3/2}$ level, we must consider thermalization in order to obtain the effective radiative lifetime of the green emission. From the radiative lifetime values reported in the literature [11], the effective transition probability at room temperature is increased by a factor of 1.3 in relation to that of the isolated $^4S_{3/2}$ level. From the effective radiative lifetime and the lifetime measurement, shown in figure 4, an efficiency in the range $\Phi = 0.18 \pm 0.02$ is obtained. This value for the luminescence quantum efficiency is substantially different from the experimental efficiency value ($\Phi = 0.31 \pm 0.05$) and the reasons for this discrepancy have to be analysed.

An additional piece of information, which has not been included in the analysis of PAS–LUMS data, is the possibility of an energy transfer process from Er^{3+} to Yb^{3+}. In fact, it has been reported that in some Er^{3+}/Yb^{3+} co-doped materials this transfer process is operative [12, 13] and therefore affects the characteristics of the green emission of Er^{3+} ions. This mechanism is possible because the energy separation between the $^4S_{3/2}$ and $^4I_{13/2}$ levels of Er^{3+} ions is only slightly larger than that between ground and excited levels of Yb^{3+} ions.

Evidence in support of the existence of this energy transfer process can be obtained through lifetime measurements, because it should affect the $^2H_{11/2}$, $^4S_{3/2}$ lifetime. The increase in the measured lifetime of the green emission of Er^{3+} ions when the Yb^{3+} ion concentration in the sample is decreased (see figure 6), reducing the transfer probability, is the proof of the existence of this process.

Therefore the analysis of the PAS and LUMS signals must be revised in order to include this additional de-excitation channel. The energy transfer process indicated above does not affect the reference channel for photoacoustic measurements and only affects the de-excitation process from the $^4S_{3/2}$ level.

Then, when the energy transfer is taken into account, the energy balance has to be reformulated and a new relationship is obtained for the luminescence quantum efficiency, which is

$$\Phi = 1 - \frac{(E_0 - E_2) - \Lambda(E_1 - E_2)}{(\Lambda - 1)(E_2 - E_3)(1 - \Psi)} \tag{4}$$

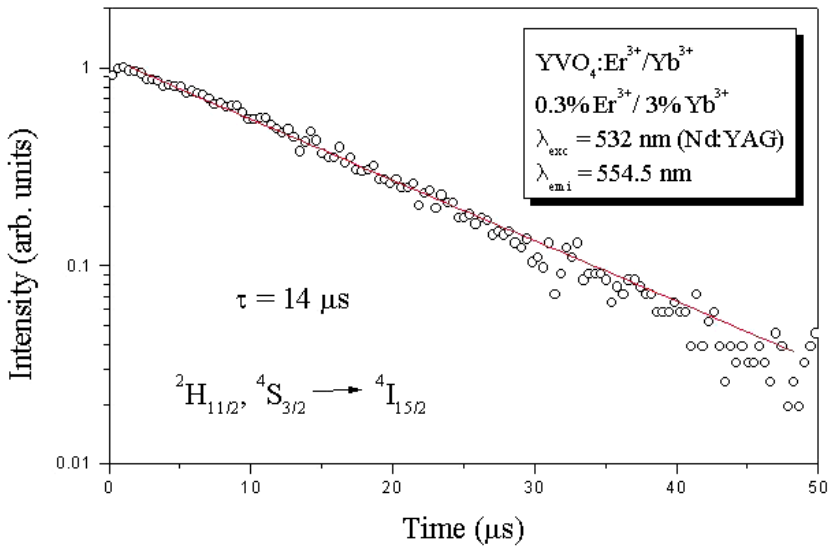

Figure 6. Temporal evolution of the green luminescence of Er^{3+} ions ($^4S_{3/2}$, $^2H_{11/2} \rightarrow {}^4I_{15/2}$), measured at 554.5 nm, after pulsed excitation of the Er^{3+} ions at 532 nm, for the sample co-doped with 3 at.% Yb^{3+} and 0.3 at.% Er^{3+} (open circles). The line corresponds to the fitting of the decay with a straight line.

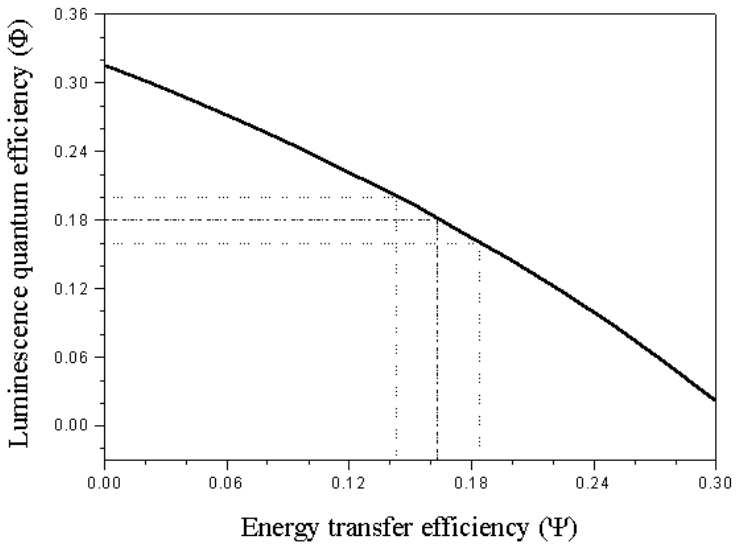

Figure 7. Relation between luminescence quantum efficiency (Φ) and energy transfer efficiency (Ψ), as given by equation (4) with $\Lambda = 2.56$.

where Ψ is the population fraction in the $^4S_{3/2}$ level, which is transferred to excited state of the Yb^{3+} ions. If Ψ is set equal to zero in this equation, which would be the case for zero transfer, equation (2) is recovered after some easy manipulation.

This equation relates the experimental value (with the two efficiencies involved in the de-excitation of the Er^{3+} ions (Φ, Ψ). The dependence between luminescence quantum

efficiency (Φ) and energy transfer efficiency (Ψ) is presented in figure 7 using the experimentally determined value $\Lambda = 2.56$. If we accept the value of the luminescence quantum efficiency evaluated from Judd–Ofelt data ($\Phi = 0.18 \pm 0.02$) the energy transfer efficiency can be inferred. From figure 7, a value $\Psi \cong 0.16 \pm 0.02$ is obtained.

In conclusion, the results indicate that in Er^{3+}/Yb^{3+} co-doped YVO_4, with a high concentration of Yb^{3+} ions, the energy transfer process ($Er^{3+} \rightarrow Yb^{3+}$) has to be considered in order to account for the dynamic population in this material. The photoacoustic and luminescence measurements are useful to obtain the efficiency of this energy transfer, which indicate that for the concentration studied in this work (10 at.% Yb^{3+} and 1 at.% Er^{3+}) 16% of the excited Er^{3+} ions transfer this energy to the Yb^{3+} ions.

Acknowledgments

Work partially supported by DGES Ministerio de Eduación y Cultura (project PB97-0019) and Comunidad de Madrid (07T/0026/1998). One of the authors (REDP) wishes to acknowledge the support by a grant from the Ministerio de Educación y Cultura of Spain. Another of the authors (TT) thanks Universidad Autonoma de Madrid for giving an opportunity to stay at the Departmento de Fisica de Materials, and also thanks Professor Ruan Yongfeng for his encouragement.

References

[1] Field R A, Birnlaum M and Finchev C L 1987 *Appl. Phys. Lett.* **51** 1885
[2] Cantelar E and Cussó F 1999 *Appl. Phys.* B **69** 29
[3] Cantelar E, Muñoz J A, Sanz-García J A and Cussó F 1998 *J. Phys.: Condens. Matter* **10** 8893
[4] Tsuboi T 2000 *Physica* B **293** 84
[5] Tsuboi T 2000 *Phys. Rev.* **62** 4200
[6] Rodriguez E, Muñoz J A, Tocho J O and Cussó F 1994 *J. Phys.: Condens. Matter* **6** 10 625
[7] Muñoz J A, Di Paolo R E, Tocho J O, Cussó F, Castañeda B, Pérez-Salas R, Aceves R and Barbosa-Flores M 1998 *J. Phys.: Condens. Matter* **10** 4113–18
[8] Muñoz J A, Di Paolo R E, Duchowicz R, Tocho J O and Cussó F 1998 *Solid State Commun.* **107** 487
[9] Muñoz J A, Herreros B, Lifante G and Cussó F 1998 *Phys. Status Solidi* a **168** 525
[10] Braslavsky S and Heihoffk S E 1989 *Handbook of Organic Photochemistry* vol 1, ed J C Scaiano (Boca Raton, FL: Chemical Rubber Company) ch 14, pp 327–54
[11] Capobianco J A, Kabro P, Ermeneux F S, Moncorgé R, Bettinelli M and Cavalli E 1997 *Chem. Phys.* **214** 329–40
[12] Okamoto E, Masui H, Muto K and Awazu K 1972 *J. Appl. Phys.* **43** 2122
[13] Mita Y, Yamamoto H, Katayanagi K and Shionoya S 1995 *J. Appl. Phys.* **78** 1219